Atherosclerosis 371 (2023) 1–13

Contents lists available at ScienceDirect

Atherosclerosis

journal homepage: www.elsevier.com/locate/atherosclerosis

# A comparative gene expression matrix in Apoe-deficient mice identifies unique and atherosclerotic disease stage-specific gene regulation patterns in monocytes and macrophages

Carmen Härdtner [a], Anup Kumar [b], Carolin A. Ehlert [a], Tamara Antonela Vico [a], Christopher Starz [a], Alexander von Ehr [a], Katja Krebs [a], Bianca Dufner [a], Natalie Hoppe [a], Peter Stachon [a], Timo Heidt [a], Dennis Wolf [a], Constantin von zur Mühlen [a], Björn Grüning [b], Clinton S. Robbins [c], Lars Maegdefessel [d,e,f,h], Dirk Westermann [a], Tsai-Sang Dederichs [a,1,**], Ingo Hilgendorf [a,g,1,*]

[a] Department of Cardiology and Angiology, University Heart Center Freiburg-Bad Krozingen, Faculty of Medicine, University of Freiburg, Hugstetter Street 55, Freiburg, Germany
[b] Department of Computer Science, Bioinformatics Group, University of Freiburg, Georges-Koehler-Allee 106, Freiburg, Germany
[c] Peter Munk Cardiac Centre, University Health Network, 101 College St, Toronto, Canada
[d] Department for Vascular and Endovascular Surgery, Technical University Munich, Arcisstr. 21, Munich, Germany
[e] Deutsches Zentrum für Herz-Kreislaufforschung (DZHK), Berlin, Germany
[f] Department of Medicine, Karolinska Institutet and University Hospital, Eugeniavägen 3, Stockholm, Sweden
[g] Institute for Experimental Cardiovascular Medicine, University Heart Center Freiburg-Bad Krozingen and Faculty of Medicine, University of Freiburg, Elsaesser Street 2Q, Freiburg, Germany
[h] Partner Site Munich Heart Alliance, Arcisstr. 21, Munich, Germany

## HIGHLIGHTS

- Aortic macrophages have the most active gene regulation during atheroma initiation.
- Inflammatory response of aortic macrophages is prominent during atheroma progression.
- Foamy macrophage marker, Gpnmb, strongly correlates with atherosclerosis advancement.
- Gpnmb $^{+}$ foamy macrophages down-regulate pro-inflammatory genes.

## GRAPHICAL ABSTRACT

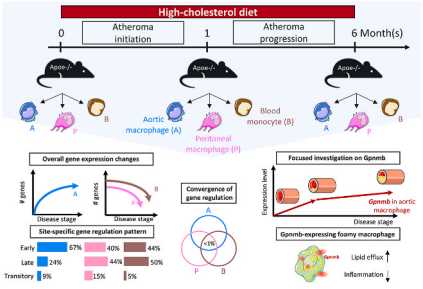


## ARTICLE INFO

*Keywords:*
Atherosclerosis
Macrophage

## ABSTRACT

*Background and aims:* Atherosclerosis is a systemic and chronic inflammatory disease propagated by monocytes and macrophages. Yet, our knowledge on how transcriptome of these cells evolves in time and space is limited.

* Corresponding author. University Heart Center Freiburg-Bad Krozingen, Dept. of Cardiology and Angiology, Hugstetter Street 55, 79106, Freiburg, Germany.
** Corresponding author. University Heart Center Freiburg-Bad Krozingen, Dept. of Cardiology and Angiology, Hugstetter Street 55, 79106, Freiburg, Germany.
*E-mail addresses:* tsai-sang.dederichs@uniklinik-freiburg.de (T.-S. Dederichs), ingo.hilgendorf@uniklinik-freiburg.de (I. Hilgendorf).
[1] These authors contributed equally to this work.

https://doi.org/10.1016/j.atherosclerosis.2023.03.006
Received 12 October 2022; Received in revised form 2 March 2023; Accepted 8 March 2023
Available online 15 March 2023

RNA-seq
Gpnmb

We aimed at characterizing gene expression changes in site-specific macrophages and in circulating monocytes during the course of atherosclerosis.
*Methods:* We utilized apolipoprotein E-deficient mice undergoing one- and six-month high cholesterol diet to model early and advanced atherosclerosis. Aortic macrophages, peritoneal macrophages, and circulating monocytes from each mouse were subjected to bulk RNA-sequencing (RNA-seq). We constructed a comparative directory that profiles lesion- and disease stage-specific transcriptomic regulation of the three cell types in atherosclerosis. Lastly, the regulation of one gene, *Gpnmb*, whose expression positively correlated with atheroma growth, was validated using single-cell RNA-seq (scRNA-seq) of atheroma plaque from murine and human.
*Results:* The convergence of gene regulation between the three investigated cell types was surprisingly low. Overall 3245 differentially expressed genes were involved in the biological modulation of aortic macrophages, among which less than 1% were commonly regulated by the remote monocytes/macrophages. Aortic macrophages regulated gene expression most actively during atheroma initiation. Through complementary interrogation of murine and human scRNA-seq datasets, we showcased the practicality of our directory, using the selected gene, *Gpnmb*, whose expression in aortic macrophages, and a subset of foamy macrophages in particular, strongly correlated with disease advancement during atherosclerosis initiation and progression.
*Conclusions:* Our study provides a unique toolset to explore gene regulation of macrophage-related biological processes in and outside the atheromatous plaque at early and advanced disease stages.

## 1. Introduction

Atherosclerosis is a chronic inflammatory disease [1–4], manifesting itself locally in atheromatous plaque growth in arterial vessels, but also systemically with increased inflammatory markers linked to elevated cholesterol levels [2,3,5–7]. Atheromatous plaque macrophages propagate disease progression primarily originating from monocytes and with unknown relations to macrophages in other compartments, such as the peritoneal cavity [8,9]. Single-cell RNA sequencing (scRNA-seq) provided major insights into macrophage subset identification in different tissues, including the atherosclerotic aorta [10–13], but typically focused on one disease stage and compartment. In this work, our objective was to compare bulk gene expression profiles of blood Ly6C$^{high}$ monocytes, aortic macrophages and peritoneal macrophages retrieved from atherosclerosis-prone mice before and during atherosclerosis development at early and advanced disease stages. We aimed to compose a unique database for therapeutic target identification and pathomechanistic investigation in experimental atherosclerosis research.

## 2. Materials and methods

### 2.1. Animals and diet

Female Apoe-deficient mice (*Apoe*$^{-/-}$, B6.129P2-Apoetm1Unc) were purchased from The Jackson Laboratory (Bar Harbor, ME, USA) and housed under specific pathogen-free conditions. At the age of eight weeks, one group of animals was sacrificed as the baseline group while the remaining mice were placed on a high-cholesterol diet (HCD, 1.25% w/w cholesterol). A second group of animals was sacrificed after four weeks of HCD to represent the early atherosclerotic disease stage, whereas the third group of animals was sacrificed after 24 weeks of HCD and having developed advanced atherosclerosis.

### 2.2. Histology

Murine aortic roots were embedded in OCT Tissue Tek (Sakura Finetek, Tokyo, Japan) and cut into serial cryostat sections (5 μm) starting at the level of the aortic valve. Sections were stained with primary antibodies anti-CD68 (clone FA-11, BioRad AbD Serotec, Purchheim, Germany), anti-Glycoprotein Nmb (GPNMB) (BS-2684R, Bioss Antibodies Inc., Woburn, Massachusetts, USA), the secondary antibodies rabbit anti-rat AF647 (ab169349, Abcam, Berlin, Germany), alpaca anti-rabbit AF488 (ChromoTek GmbH, Planegg-Martinsried, Germany), and DAPI Mounting Medium (Carl Roth, Karlsruhe, Germany) according to the manufacturers' instructions. Abdominal aortas were pinned for Oil-red O (ORO, Sigma Aldrich, St. Louis, MO, USA) en face staining. Fluorescent images were recorded with the Axioplan 2 imaging fluorescence microscope (Carl Zeiss MicroImaging GmbH, Göttingen, Germany). Images were analyzed with Image Pro Premier 9.2 (Media Cybernetics, Silver Springs, USA).

### 2.3. Cholesterol assay and enzyme-linked immunosorbent assay (ELISA)

Murine plasma cholesterol levels were measured using Cholesterol FS 10′ Multi-purpose kit (DiaSys Diagnostic Systems GmbH, Holzheim, Germany) according to the manufacturer's instructions. Murine plasma samples for mouse GPNMB ELISA (ab270892, Abcam Berlin, Germany) were diluted 1:10 and the assay was performed following manufacturer's instructions.

### 2.4. Stable and unstable human plaque

Human plaque specimens were provided from patients with carotid artery disease undergoing carotid endarterectomy at the Department of Vascular and Endovascular Surgery at the Klinikum rechts der Isar of the Technical University Munich, Munich, Germany. All patients provided written informed consent, and the study has been approved by the local Ethics committee at the Klinikum rechts der Isar of the Technical University Munich. Plaque stability was assessed using the Rothwell/Redgrave criteria based on fibrous cap thickness (>200 μm stable, <200 μm unstable) on hematoxylin & eosin stained slides as previously shown [14,15].

### 2.5. RNA isolation and sequencing

Aortic macrophages, peritoneal macrophages, and pooled monocytes from blood and spleen were sorted directly into Buffer RLT (QIAGEN, Stockach, Germany) plus 1% β-mercaptoethanol (AppliChem, Darmstadt, Germany). After further homogenizing the cell lysates with QIAshredder (QIAGEN, Stockach, Germany), we extracted the RNA from the lysates with RNeasy Micro kit (QIAGEN, Stockach, Germany). We prepared RNA library with the Ovation SoLo RNA-seq systems (NuGEN, Crailsheim, Germany). The library was sequenced on a NextSeq instrument with 75 bp paired-end reads using NextSeq 500 High Output v2 kit (Illumina, San Diego, CA, USA). At least 2.5 million reads were acquired from each bulk sample.

### 2.6. Bioinformatic processing of RNA-seq data

The transformation of fastq files to gene counts was processed in the Galaxy platform (https://usegalaxy.eu/). After ensuring adequate quality using FASTQC (Galaxy Version 1.7), cutadapt (Galaxy Version 1.16.5) was used to trim adapters and end bases with Phred score lower

than 20. Applying the criteria, all samples had less than 2% reads trimmed. Trimmed reads with length shorter than 20 bp were discarded. The trimmed reads were aligned to the mouse genome (mm10) using RNA STAR (Galaxy Version 2.7.2b) with default settings. At least 1.7 million uniquely aligned reads were acquired from each sample. FeatureCounts (Galaxy Version 1.6.4+galaxy1) was applied to count the features from the forward stranded bam files using default settings. All samples had at least 1.1 million reads assigned to a feature. The gene count files were downloaded and imported into R (Version 4.0.4) for downstream analyses.

### 2.7. Bioinformatic analysis of differentially expressed genes, regulation patterns, and gene ontology (GO) enrichment

We utilized dplyr (Version 1.0.7) to compute the gene count files. Expressed genes were defined as genes expressed in at least 3 out of 4 biological replicates. Differentially expressed genes (DEGs) were called by DESeq2 (Version 1.28.1). Significantly regulated genes were genes that increased or decreased significantly as opposed to earlier disease stages. DEGs of each cell type were grouped into early, late, and transitorily regulated genes based on their regulation patterns. The grouped DEGs were used for the enrichment analysis of biological pathways with clusterProfiler (Version 3.16.1). Statistical significance of DEGs and enriched pathways were defined as adjusted $p$-value $<0.05$ post-Bonferroni correction.

### 2.8. Bioinformatic inspection of Gpnmb expression in scRNA-seq datasets

Single-cell gene expression matrices and metadata were retrieved from Gene Expression Omnibus (GEO) dataset GSE131776 or offered by the authors [12,16]. From GSE131776, only *Tcf21* wild-type samples were utilized in our analysis as previously described [17]. The *Apoe*$^{-/-}$ mouse datasets were analyzed jointly with Seurat (version 4.0.3). In short, the raw counts were logarithmically normalized with the scale factor of 10,000; thereafter, the 2000 most variable genes identified with variance stabilization transformation were used in principle component analysis. With RunUMAP, the first 20 principle components were applied for dimensionality reduction. Graph-based clustering was performed by FindNeighbors and FindClusters with a resolution of 0.65 and 1.2 for the GSE131776 and Winkels et al. datasets, respectively [12]. Cell types were appointed to the clusters based on the markers suggested in both publications. The combined matrices and metadata with cell type information were made into a Seurat object and analyzed according to the standard Seurat workflow with all parameters kept the same except that the resolution was fine-tuned to 0.8 for clustering. The two datasets were nicely integrated that the macrophage and T cell clusters from both sources lapped over. For the simplicity of presentation, we dismissed the subcluster annotation of smooth muscle cells and T cells. The macrophage subset was extracted from the Seurat object and underwent the standard Seurat workflow with the aforementioned parameters. Subtypes of macrophage were identified and annotated according to the known markers—inflammatory (*Tnf*, *Il1b*, and *Ccl3*), resident-like (*Folr2*, *Timd4*, *Lyve1*)), and foamy (*Lgals3*, *Cd9*, and *Trem2*)) [12,16]. We further analyzed the combined macrophage matrix and metadata with FindIntegrationAnchors and IntegrateData functions, following the Seurat v3 Integration workflow. From GSE131776, we acquired the human right coronary artery single-cell dataset and integrated the data by RunHarmony (v1.0) to remove the inter-individual variables. Thereafter, we used the same analysis workflow and settings that we applied to the mouse datasets. Comparison of gene expression in *Gpnmb*$^{+}$ and *Gpnmb*$^{-}$ foamy macrophages was performed using permutation test. From GSE159677, we acquired single-cell macrophage data of human carotid plaque retrieved from atherosclerotic core and proximal adjacent tissue. The data was analyzed using the same workflow applied to GSE131776 dataset.

### 2.9. Data visualization

All cell types acquired at different disease phases were clustered based on principle component variances and visualized with plotPCA of DESeq2 package (Version 1.28.1). Number of genes present in various compartments throughout the disease course was visualized by Sankey diagram using plotly (Version 4.9.4.1) and by Venn diagram using colorfulVennPlot (Version 2.4). The color scale of grid plot was made with ggplot2 (Version 3.3.5). Logarithmic mean counts of highly differentially regulated genes were shown in heatmaps with pheatmap (Version 1.0.12). Graphs of single-cell datasets were programmed with Seurat (Version 4.0.3). The dimensional reduction plots were generated with DimPlot. The Expression of features and *Gpnmb/GPNMB* was visualized by FeaturePlot and VlnPlot.

### 2.10. Data availability

The datasets supporting the conclusions of this article are available in the GEO database repository, GSE213189, GSE131776, GSE159677 and GSE213189, and enclosed within the article and its Supplementary Table A.2.

## 3. Results

### 3.1. Compartment-determined myeloid cell transcriptomic profiles in Apoe-deficient mice

At eight weeks of age with modestly elevated cholesterol levels on a chow diet, aortas from *Apoe*$^{-/-}$ mice were free of atherosclerotic lesions in en face lipid staining of the aorta. One month after the start of HCD, we observed an 7.7% (95% confidence interval (CI): 5.7%–9.0%) lipid coverage in the aortic inner layer, which indicated an early formation of atheroma. Atherosclerosis advanced as HCD feeding was continued for another 5 months accelerating hypercholesterolemia and covering about 30.7% (95% CI: 29.3%–31.4%) of the aortic surface with lipid-rich plaques (Fig. 1A–C).

To understand the transcriptomic regulation of atheroma-associated macrophages, we performed bulk RNA-seq of F480$^{high}$ macrophages isolated from thoracoabdominal aortas of mice representing different stages of atherosclerosis: baseline (absence of disease), early and advanced disease. From the same animals, we collected another two cell populations as comparators: First, pooled Ly6C$^{high}$ monocytes isolated from blood and spleen, which represent major precursor cells of atheromatous plaque macrophages that proliferate in situ [18,19]. Second, peritoneal macrophages which settled in a compartment distant from the aortic lesion. These cells are still exposed to systemic hypercholesterolemia and regularly being used for foam cell formation studies [20–22]. For the simplicity of presentation, and given that gene expression profiles of splenic reservoir monocytes overlap with those of circulating blood monocytes [23], the source of monocytes is labeled as blood in the rest of the text. The three myeloid cell populations sorted from four *Apoe*$^{-/-}$ mice per group at the three time points of atherosclerosis development were subjected to RNA-seq (Fig. 1D, Supplementary Fig. 1).

The RNA-seq results revealed an overall high-quality data with a mean Phred score of above 25 for all nucleobases of the trimmed reads. Raw sequencing reads were converted to gene counts following genome alignment and feature counting. With principal component analysis, we identified three clusters which were distinctively separated according to the compartments where the cells were retrieved from. Sub-grouping associated with disease stages was observed in macrophages in particular (Fig. 2A, Supplementary Fig. 2). The finding suggested that the compartmentalized environment played a dominant role in shaping cell biology despite systemic exposition to hypercholesterolemia throughout atherosclerotic disease development. Yet, comparing gene expression profiles between all three cell types at three disease stages identified

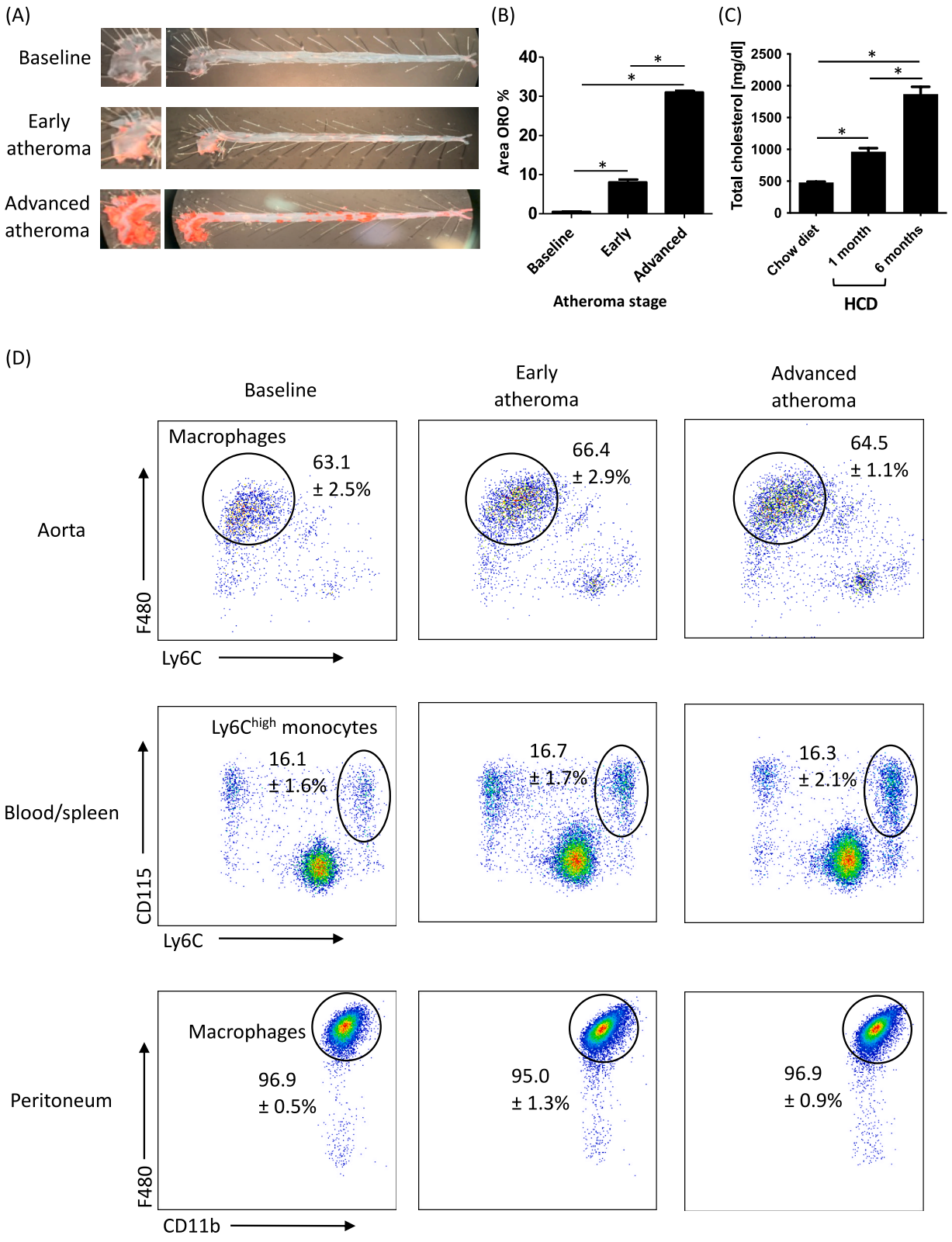


**Fig. 1.** Severity of atherosclerosis of the studied mice and the isolation of monocytes and macrophages for bulk RNA-seq.
(A) Representative pictures of ORO-stained aorta of mice undergoing zero, one, and six months of HCD feeding. (B and C) Quantification of lipid deposition in aorta by area covered by ORO, and of total cholesterol in plasma. Results are presented as mean ± SEM, *$p < 0.05$ denotes statistically significant differences between groups, n = 4 per group, One-way ANOVA with Holm Sidak Post-hoc testing. (D) Representative dot plots of flow cytometry bulk-sorting gates. The framed area in each plot encircles sorted cells with their respective mean percentages ± SEM. 451.8 ± 115, 1688 ± 337.8 and 5912 ± 1836, *, §aortic macrophages were sorted at baseline, early and advanced disease stages, respectively. Counts are presented as mean ± SEM, n = 4 per group, *, § $p$-value $< 0.05$ denotes statistically significant differences between baseline and early (*), and early and advanced (§) groups, One-way ANOVA with Holm-Sidak *post-hoc* testing. For blood/splenic monocytes and peritoneal macrophages, 50.000 cells each were sorted. Four mice were used per condition.

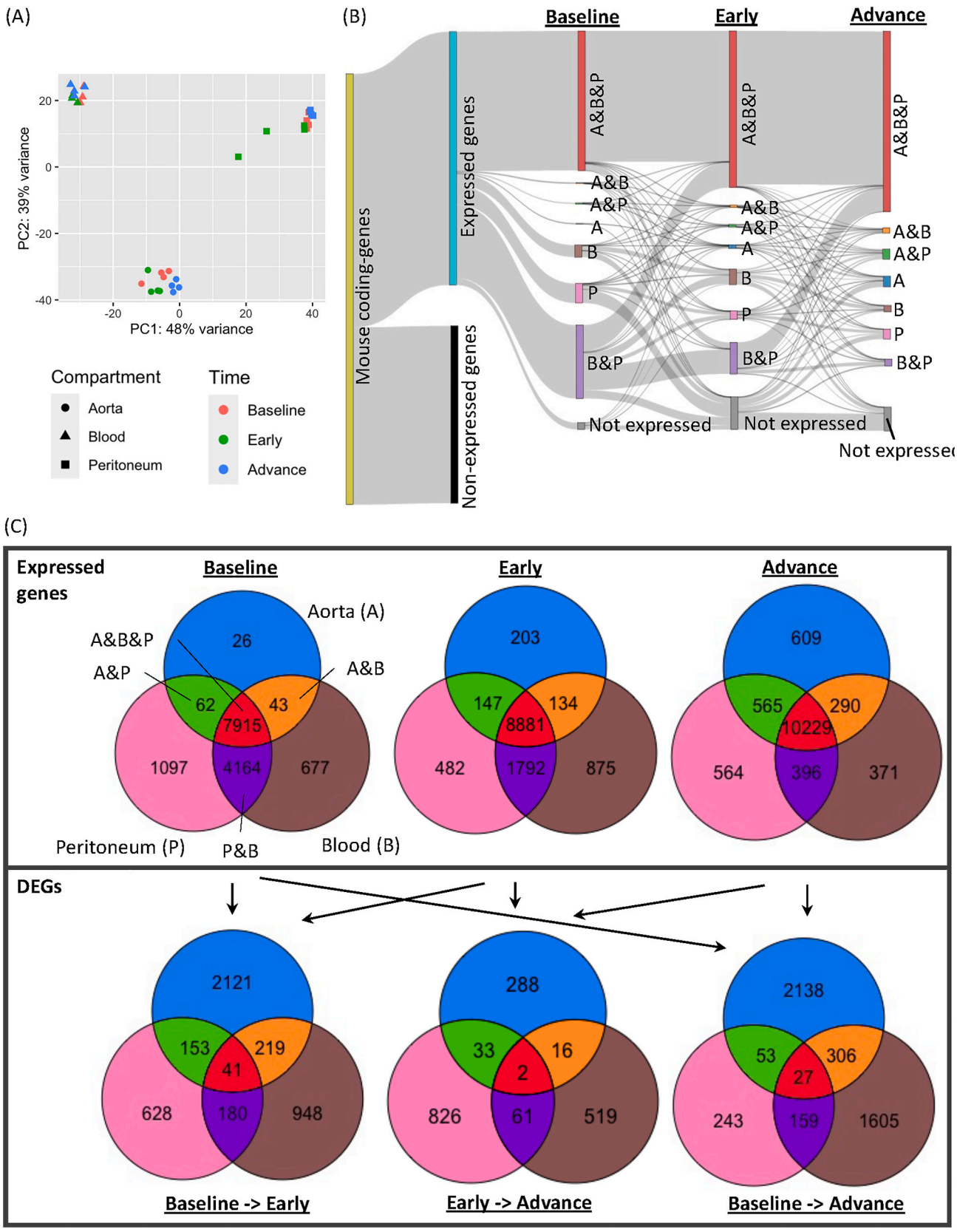


**Fig. 2.** Gene expression and regulation according to disease stages and physical compartments of monocyte/macrophages.
(A) Principle component analysis (PCA) plot of all samples undergoing bulk RNA-seq. (B) Sankey plot depicting quantitative changes of expressed genes in monocytes or macrophages of single or shared compartments at different stages of atherosclerosis. (C)Venn diagrams showing the number of expressed genes (upper) and DEGs (lower) in monocytes or macrophages of single or shared compartments at different stages of atherosclerosis. A, aorta; B, blood; DEG, differentially expressed gene; P, peritoneum; n = 4 per group.

hundreds to a few thousand DEGs even within the same compartment (Supplementary Fig. 3). We therefore asked: to what extent a common hypercholesterolemic challenge would incite similar or unique gene expression changes in the three myeloid cell populations during atherosclerosis initiation and progression.

### 3.2. Shared and differentially regulated genes in monocytes and macrophages during atherosclerosis

The studied monocytes and macrophages of all disease stages expressed overall 14362 genes among 24421 annotated genes. Most of the genes were commonly expressed by all three cell types, irrespective of disease stages, accounting for the housekeeping genes required for basic cellular functions (Fig. 2B and C). At baseline, only few genes were expressed exclusively in aortic macrophages, whereas thousands of genes were expressed uniquely or shared in blood monocytes and peritoneal macrophages. During the course of atherosclerosis, however, we observed a continuous increase of genes expressed in the aortic macrophage cell population; in contrast, the number of genes exclusively present in blood monocytes or peritoneal macrophages declined, many of which were later commonly shared by aortic macrophages. These observations are in line with the prevailing concept that infiltrating monocytes are the primary source of atheromatous plaque macrophages (Fig. 2B). At the advanced disease stage, 609 genes were uniquely expressed in aortic macrophages. Testimony to a compartment-specific transcriptomic regulation, this number exceeded those in monocytes and peritoneal macrophages (Fig. 2C). The compartment-specific transcriptomic regulation was even better illustrated by the number of DEGs during atherosclerosis development (Fig. 2C). Supplementary Fig. 4 illustrates how the number of genes in the Venn diagrams were counted.

Hundreds of DEGs were uniquely regulated in each of the three compartments, whereas only a maximum of 41 DEGs were commonly shared (Fig. 2C, Supplementary Table A.1). The number of DEGs at different disease stages also varied noticeably between the compartments (Fig. 2C). In both macrophage populations, more genes were upregulated than downregulated early during atherosclerosis development; whereas in blood monocytes or during disease progression, up- and downregulation of genes was more evenly distributed (Supplementary Fig. 5A). Supplementary Fig. 5B shows a selected panel of genes that were highly expressed in a stage-specific manner, exemplifying variable patterns of gene regulation, which show consistent or transient up- or downregulation during disease progression. Next, we categorized all DEGs according to their regulation patterns as being regulated early, transitorily or late during atherosclerosis development to explore disease stage- and compartment-specific functions based on gene expression changes.

### 3.3. Monocyte/macrophage populations feature divergent gene regulation patterns during atherosclerosis

Fig. 3 summarizes the overall regulation pattern of each gene in each compartment, which are listed in detail in Supplementary Table A.2. Aortic macrophages carried 11845 expressed genes, among which 3245 genes were differentially regulated throughout the disease course. To our surprise, although we identified thousands of DEGs in aortic macrophages, only ten of them were continuously upregulated during atheroma initiation and progression. All of these genes were lowly expressed or downregulated in blood monocytes and peritoneal macrophages, demonstrating a unique gene regulation in the atheroma lesion. The majority of DEGs in macrophages (n = 1729) isolated from aortas with early atherosclerotic lesions showed an increased expression which did not change significantly during disease progression. Conversely, 80 genes were downregulated early on and remained suppressed in macrophages from advanced atheroma. Together, more than half of the DEGs in aortic macrophages were regulated early during atherogenesis. Twenty-two percent of aortic macrophage DEGs were regulated transitorily, meaning that they showed either an increased (n = 207) or decreased (n = 508) expression level at the early disease stage compared to baseline, which was subsequently reverted as no significant gene expression change was detected at the advanced disease stage relative to baseline. Another twenty-two percent of aortic macrophage DEGs were regulated late, meaning that they showed an increased (n = 450) or decreased (n = 135) expression level at the advanced but not the early disease stage compared to baseline. Only 126 aortic macrophage DEGs were significantly regulated during progression of atherosclerosis from early to the advanced disease stage. In contrast, 43% of peritoneal macrophage DEGs and 52% of blood monocyte DEGs featured a late regulation pattern (Fig. 3).

Thus, during atherogenesis, nearly 80% of gene expression changes in aortic macrophages occur within 4 weeks of disease onset in *Apoe*$^{-/-}$ mice on HCD. About a quarter of these regulated genes reverted their expression changes during further disease progression. Blood Ly6C$^{high}$ monocytes regulated hundreds of genes as cholesterol started to accumulate in the circulation, but most of their expression changes occurred gradually over time and reached statistical significance at the advanced disease stage only. In peritoneal macrophages, which situated distant from the atherosclerotic aorta, most genes were regulated transitorily. In aortic macrophages, however, the most frequent regulation pattern was an early upregulation of DEGs which remained uplifted during disease progression. In peritoneal macrophages, which situated distant from the atherosclerotic aorta, transitory regulation was the most frequent in this cell type, whereas in aortic macrophages, the most frequent regulation pattern was an early upregulation of DEGs which remained uplifted during disease progression. As shown in Fig. 2c, only 41 out of 4290 genes were regulated in common by all three cell populations during initiation of atherosclerosis, and nearly none later on. Notably, gene regulation patterns differed even in those few shared DEGs between compartments (Supplementary Table A.1). Given the obvious differences in gene regulation patterns between the cell populations and considering the small overlap in shared DEGs, we interrogated the functional implications of gene expression changes in each compartment.

### 3.4. Compartments determine monocyte and macrophage functions in atherosclerosis

DEGs grouped as regulated early, transitorily and late were enriched in variable biological processes according to GO term analysis. Our data revealed that in the aorta, DEGs regulated early enriched biological processes that related to general cellular responses to stress, such as apoptosis and autophagy, as well as to extracellular matrix remodeling of the plaque microenvironment with collagens and metalloproteinases. Common macrophage features, such as inflammation, lipid handling, and macrophage activation were manifested by DEGs regulated transitorily or late (Fig. 3). On the contrary, biological processes associated with immune activation were enriched in Ly6C$^{high}$ monocytes early on, where leukocyte migration and myeloid cell differentiation were key procedures that monocytes require to infiltrate and form atheroma lesions. Peritoneal macrophages, distant from the lesion site, had a mild response during atheroma initiation shown by the low number of early-regulated DEGs with enriched biological process unspecific to immune reactions. However, a systemic impact was revealed by their late-regulated DEGs, which involved NFκB signaling, macrophage activation, and TNF family cytokine production (Fig. 3).

The gene regulation patterns and enriched biological processes suggest that compartments determined monocyte and macrophage reactions in a disease stage-specific manner. During atheroma initiation, circulating monocytes prepared to migrate and differentiate. At the same time, macrophages in the aorta showed cellular response to stress as well as secretory factors for extracellular matrix organization, an essential atherogenic procedure which promotes cell proliferation and migration [18,24,25]. All three cell types showed inflammatory

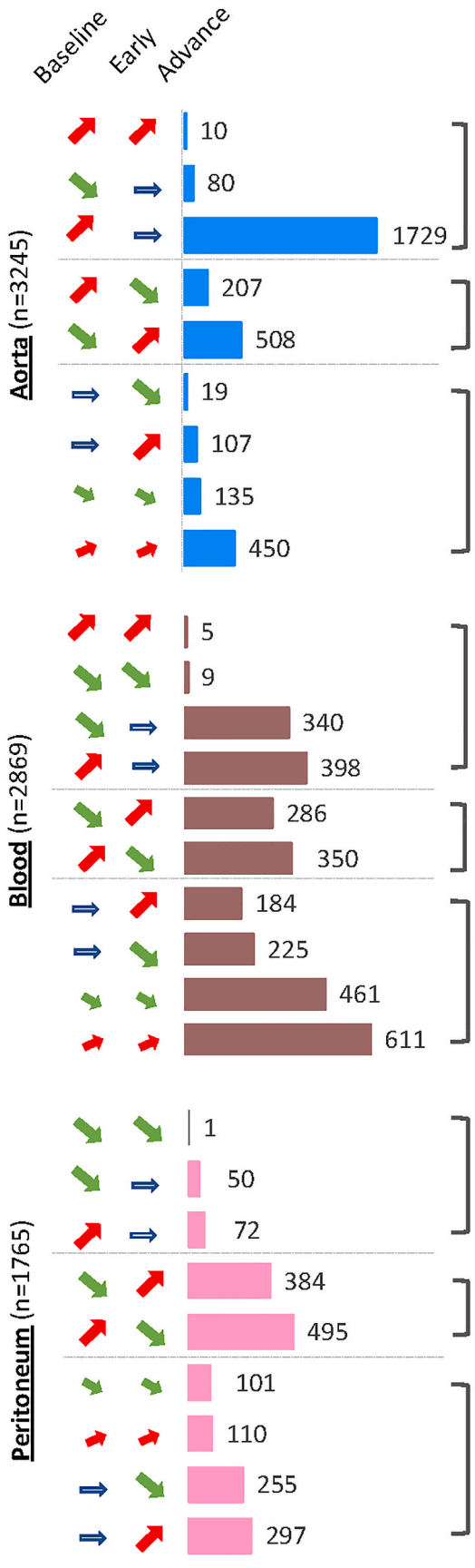


**Biological processes uniquely enriched in different disease stages**

- Extracellular matrix organization (17.3)
- Response to oxidative stress (13.5)
- Regulation of apoptotic signaling pathway (12.3)
- Regulation of mitotic cell cycle (11.4)
- Autophagy (11.1)

- Regulation of IFNγ production (11.0)
- Regulation of lipid transport (8.9)
- Regulation of TNF cytokine production (7.8)
- Positive regulation of cytokine production (7.3)

- Regulation of IL1 production (13.2)
- Cellular response to IL1 (12.0)
- Macrophage activation (10.8)
- Response to TGFβ (9.3)
- Regulation of cell growth (7.2)

- Response to TGFβ (9.6)
- Myeloid cell differentiation (9.2)
- Leukocyte migration (7.9)
- I-kappaB kinase/NF-kappaB signaling (7.3)
- Phagocytosis (7.1)

- IFNγ production (13.9)
- Leukocyte cell-cell adhesion (12.2)
- Positive regulation of cytokine production (7.8)

- Positive regulation of cytokine production (14.4)
- Myeloid cell differentiation (12.0)
- Autophagy (11.9)
- Response to oxidative stress (11.3)
- Lipid transport (10.9)
- Phagocytosis (10.1)

- Positive regulation of G1/S transition of mitotic cell cycle (10.3)
- Cytoplasmic translation (9.6)

- Regulation of cell-cell adhesion (12.2)
- Leukocyte proliferation (9.3)
- Regulation of apoptotic signaling pathway (8.2)
- Positive regulation of cytokine production (8.0)

- I-kappaB kinase/NF-kappaB signaling (10.4)
- Phospholipid biosynthetic process (9.5)
- Macrophage activation (9.6)
- TNF superfamily cytokine production (8.8)
- Receptor-mediated endocytosis (8.6)
- Regulation of mitotic cell cycle (7.5)

*(caption on next page)*

**Fig. 3.** Frequency of regulation patterns of the DEGs and the enriched biological processes based on disease stages.
Bar charts showing the frequency of regulation patterns of the DEGs of each monocyte or macrophage compartment. Colored arrows indicate the regulation direction and the statistical significance, based on which we could assign each DEG a regulation pattern. The regulation patterns were further categorized into three groups, regulated early, late, and transitorily. Genes belonging to the same group of each monocyte or macrophage compartment were used for biological process enrichment analysis. Statistically enriched biological processes that were uniquely identified in a specific disease stage were listed in the shaded boxes right next to the gene group. Statistical significance of DEGs and enriched pathways were defined as adjusted $p$-value $< 0.05$ post-Bonferroni correction (n = 4 per group). Number in the brackets next to the GO terms indicate the ratio of DEGs to all genes composing the GO term.

reactions by genes regulated transitorily or late, revealing a sustained systemic inflammation during atheroma progression. Nevertheless, we observed a more intensive immune response in the atheroma lesion as opposed to the systemic compartments (Supplementary Fig. 6).

Compared to circulating monocytes and peritoneal macrophages, aortic macrophages had higher expression of genes associated with cell proliferation and immune activation, such as cytokines and toll-like receptors (Fig. 4A). In general, monocytes had lower expression of chemokines and genes related to lipid handling than macrophages did. Having said that, aortic and peritoneal macrophages showed a distinctive regulation of phagocytic receptors. For instance, aortic macrophages had a higher expression of *Trem2*, whereas peritoneal macrophages expressed more *Msr1* (Fig. 4A). Both of these two genes function in lipid uptake and thus contribute to atherogenesis [10,26]. However, our data illustrated a distinctive expression and regulation of these two genes in compartmentally segregated macrophages from the same atherosclerotic organisms, elucidating macrophage reactions depending on their microenvironment. Indeed, although macrophage activation (GO:0042116) was an enriched biological process in all three investigated cell types, only few involved genes were actually shared by all cell types. Fig. 4B illustrates the DEGs and their regulation patterns in the three cell types, presenting disparities of gene regulation between monocytes and macrophages from different compartments. In addition, most of genes involved in aortic macrophage activation were constantly upregulated, whereas many DEGs controlling macrophage activation in circulating monocytes and peritoneal macrophages were transitorily regulated. A similar pattern of gene regulation discrepancy was observed in the production of IL-1β (GO:0032611) (Supplementary Fig. 7), suggesting a continuous pro-inflammatory reaction in the aorta as opposed to a fluctuating inflammatory response in compartments distant from the atheroma lesion.

### 3.5. Multifaceted validation of Gpnmb expression and its association with atheroma development

To validate our RNA-seq directory and to demonstrate the applicability of our RNA-seq directory in generating pathomechanistic and therapeutic insights, we inspected the expression of Gpnmb in murine and human atheroma, using published scRNA-seq datasets. We selected *Gpnmb*, because it was one of the ten DEGs that significantly up-regulated between each of the disease stages. *Gpnmb* was previously reported in association with neuroinflammation and liver damage involving organ-specific macrophages; however, controversial data assert that *Gpnmb* functions to promote as well as resolve inflammation [27]. *Gpnmb* was also identified as one of the markers of foamy macrophages in atheroma plaques [10] and it is present in extracellular spaces, either secreted or cell membrane-bound [28]. The features mentioned above made *Gpnmb* a suitable candidate for demonstrating the practicality of our directory using multifaceted molecular biology tools.

During the course of atherosclerosis, the total counts of *Gpnmb* remained low with subtle changes in blood monocytes and peritoneal macrophages, whereas aortic macrophages up-regulated *Gpnmb* by 220 and 50 folds during atheroma initiation and progression, respectively (Fig. 4A). The disease stage-, and compartment-dependent elevation of *Gpnmb* was confirmed with real-time polymerase chain reaction (PCR). (Supplementary Fig. 8A). The profound change of gene expression suggested its positive association with atheroma development, which was also reflected by an increase in Gpnmb protein levels in the plasma of *Apoe*$^{-/-}$ mice as atherosclerosis progressed (Supplementary Fig. 8B).

To further understand the correlation of *Gpnmb* and atherosclerosis, we investigated scRNA-seq datasets acquired from atherosclerotic aortas of *Apoe*$^{-/-}$ mice [12,16,17]. We observed that *Gpnmb* was almost exclusively expressed in fibroblasts and some macrophages. A similar cell type-specific expression was also shown in human plaques (Fig. 5A and B). Subsequently, we had a closer look at macrophage subtypes classified by the hallmark genes for foamy, inflammatory, and resident-like macrophages, as previously described [17,29,30] (Supplementary Fig. 9). The analysis revealed that *Gpnmb* was distinctively expressed by *Trem2*$^{+}$ foamy macrophages in both mouse and human plaque (Fig. 5C and D). Furthermore, the data suggested that an escalation of *Gpnmb* expression within a heterogeneous pool of aortic macrophages likely resulted from a growing fraction of foamy macrophages within advancing atherosclerotic lesions as opposed to an unanimous upregulation of *Gpnmb* by all aortic macrophages. In line, thin-cap unstable atheroma with a large lipid core expressed numerically higher tissue *Gpnmb* levels compared to thick-fibrous cap atheroma in humans (Supplementary Fig. 10).

On a single-cell level, *Gpnmb*-expressing foamy macrophages expressed higher levels of lipid flux genes (e.g. *Trem2*, *Abca1*, *Abcg1*, *Lrp1*, and *Cd36*) but lower levels of pro-inflammatory genes (e.g. *Nfkbia*, *Tnf*, *Nlrp3*, and *Il1b*) as opposed to murine foam cells not expressing *Gpnmb*. Peroxisome proliferator activator activated receptor gamma (*Pparg*), a ligand-activated transcription factor that reduces inflammatory response and stimulates cholesterol efflux [31] was overexpressed in *Gpnmb*$^{+}$ foamy macrophages (Fig. 5E). A similar phenotype of *GPNMB*$^{+}$ foamy macrophages was observed in humans, in particular with regard to the lipid flux features and suppressed pro-inflammatory markers (Fig. 5F). Histological staining of aortic roots from atherosclerotic *Apoe*$^{-/-}$ mice verified the expression of Gpnmb protein in a small fraction of CD68$^{+}$ macrophages residing in the plaque (Fig. 5G) in a range similar to the fraction of *Gpnmb*$^{+}$ macrophages detected in the scRNA-seq dataset (Fig. 5C). Comparing scRNA-seq data [32] of human macrophage populations isolated from the atherosclerotic core to those retrieved from the adjacent, less diseased section of the same atheromatous plaque, we observed elevated *GPNMB* expression in the atherosclerotic core predominately by *Trem2*$^{+}$ foamy macrophages (Fig. 5H). Thus, to the extent that different regions within the same human plaque can reflect atherosclerotic disease progression, the stage-dependent rise in *Gpnmb* expression in our murine aortic macrophage time line analysis well aligned with the human data.

## 4. Discussion

Our directory provides an overview of transcriptomic regulation of macrophages in the course of atherosclerosis. Monocytes and macrophages collected via fluorescence-activated cell sorting (FACS) in our directory were defined based on the long-established surface markers, which streamlines the cross-comparison of our dataset with most published works as well as the extrapolation of our findings. To acquire a comprehensive view of gene regulation in a defined cell group, bulk RNA-seq is the current method of choice as it retains most transcriptomic information in a cost-effective fashion. Nevertheless, we are aware of the compromise of identifying cell subpopulations by our method, whereas alteration of macrophage biology within atheroma were still evidently manifested in our dataset.

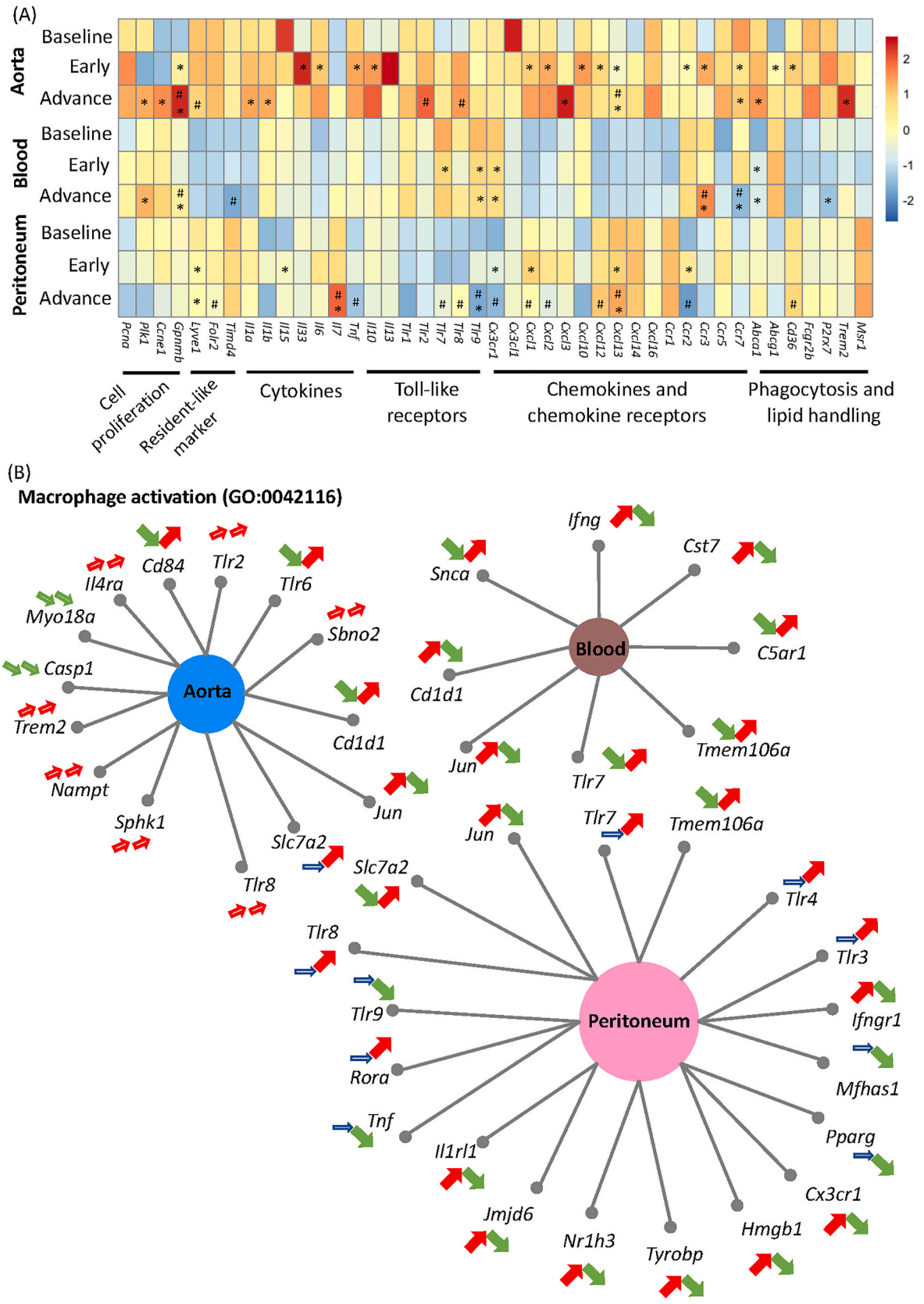


**Fig. 4.** Aortic macrophages uniquely upregulated genes associated with inflammation and lipid handling.
(A) Heatmap showing mean expression of genes relevant to macrophage function in atherosclerosis (n = 4 per group). * and # denote adjusted *p*-value < 0.05 (post-Bonferroni correction) compared to baseline and early disease stage of the same cell type, respectively. (B and C) Network plot showing genes that enriched biological process of macrophage activation in each monocyte or macrophage compartment. Arrows alongside the genes indicate their regulation pattern.

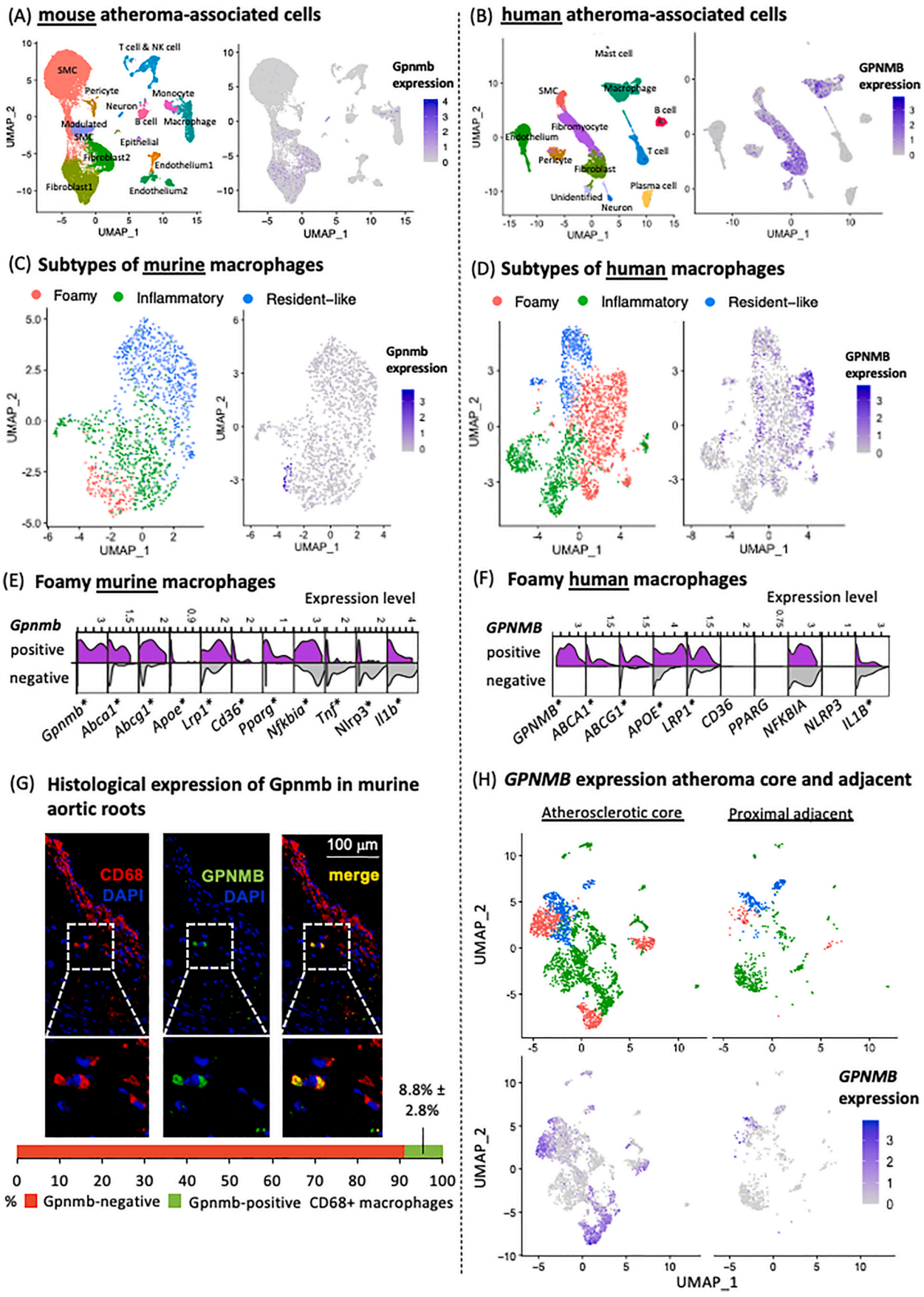


*(caption on next page)*

**Fig. 5.** Regulation of GPNMB in atherosclerotic aorta of mouse and human.
(A and B) Uniform Manifold Approximation and Projection (UMAP) plot showing atheroma-associated cells and *Gpnmb* expression in mouse and human. (C and D) UMAP plot showing subtypes of macrophages and the expression of *Gpnmb* in mouse and human. (E and F) Stacked violin plots showing the expression of genes related to efferocytosis and inflammation in *Gpnmb*$^{+}$ and *Gpnmb*$^{-}$ macrophages. (G) Representative histology image with co-staining of nucleus, CD68$^{+}$ macrophages, and Gpnmb in murine aortic root lesions. Bar chart showing the proportion of Gpnmb$^{+}$ CD68$^{+}$ macrophages of three mice, from each of which, 10 to 11 sections were used for quantification (mean ± SEM). (H) UMAP plot showing *GPNMB* expression in subtypes of macrophages retrieved from atheromatic core or proximal adjacent human plaque. CD, cluster of differentiation; DAPI, 4′,6-diamidino-2-phenylindole; Star signs indicate *p*-value < 0.05 by permutation test.

### 4.1. Evident and specific capture of compositional change of aortic macrophage population by bulk RNA-seq

The continual discovery of diverse origins of aortic macrophages has been fascinating the community over decades [10,12,33–35]. Recruited monocytes have long been considered the only source of aortic macrophages [36–38]. They infiltrate the atherosclerotic lesion, differentiate into macrophages, and trigger the inflammation cascade [19], which was reflected by the time-dependent elevation of chemokines (*Ccl2*, *Ccl3*, *Cxcl2*) [39] and inflammation markers (Il1a, *Il1b*, *Il6*, *Tnf*) [25] recorded in our directory. Resident-like macrophages, on the other hand, plausibly proliferated in proportion to the atheroma plaque advancement, indicated by a rather steady expression of its hallmark genes (*Lyve1*, *Folr2*, *Timd4*) throughout the disease course (Fig. 4A). We previously demonstrated that local proliferation of macrophages also contribute to atheroma expansion in *Apoe*$^{-/-}$ mice that received two to six month of HCD [17–19], and accordingly cell proliferation markers were upregulated in aortic macrophages (Fig. 4A). Vascular smooth muscle cell-transdifferentiated macrophage-like cells were absent in our macrophage pool due to the exclusion of *Cd45*-negative cell populations during FACS sorting. The hallmark cell type of atherosclerosis, Trem2$^{+}$ foamy macrophages, undoubtedly emerged in the growing atheroma [40,41]. Importantly, the aforementioned features were only revealed in macrophages isolated from aorta but not in those collected from peritoneum, which demonstrates an adequate capture of macrophage transcriptomic regulation in lesional and distant compartments both being exposed to hypercholesterolemia. Because the full murine aorta was subjected to bulk RNA-seq, macrophages presenting with resident cell-like features may stem from both the adventitia and intima. However, also human atherosclerotic plaque free of adventitial tissue contain resident-like macrophages, and we therefore consider resident-like macrophages in the intimal plaque as relevant for disease. The advancement of single-cell technologies enables the subtyping of atheroma macrophages to an unprecedented granularity [10,12,42–45], which supports an in-depth understanding of macrophage evolution in the atheroma lesion. However, surface markers of many of these macrophages are not fully established, thus limits the use of bulk RNA-seq to study specific subtypes of macrophages. On the other hand, it is more cost-efficient to study larger number of samples using bulk RNA-seq. Considering study granularity and affordability, we consider that bulk and single-cell RNA-seq methods compensate each other and should be exploited according to the research questions.

### 4.2. Selection of suitable macrophage targets with minimal extra-aortic effects

Using anti-inflammatory agents to combat atherosclerosis is currently an area of research [46–48]. Our data also supports this strategy as many pro-inflammatory cytokines (*Il1a*, *Il1b*, *Il6*, *Tnf*) were expressed more strongly by macrophages in aorta than by those in peritoneum. Facilitation of reparative macrophages also appears propitious, especially in the advanced atheroma. We found that the anti-inflammatory cytokines, *Il13* and *Il33* [49,50] reached their highest expression in the early phase and dropped in the advanced atheroma (Fig. 4A), indicating that failing to sustain anti-inflammatory effects might deteriorate atherosclerosis. According to our dataset, we propose a more cautious monitoring of using therapeutics that target LDL receptors on monocytes and macrophages, because these cells downregulate LDL receptor expression in the course of atherosclerosis, which could possibly result in treatment ineffectiveness overtime. However, targeting scavenger receptors appears as more adequate approach for targeting lipid-laden macrophages, the hallmark cell type of atheroma [18,51–53]. Among the long list of scavenger receptors, our dataset provides some hints that assist target prioritization. *Trem2* appears the most favorable target because of its time-dependent upregulation in aortic macrophages and low expression in peritoneal macrophages (Fig. 4A). Conversely, *Cd36* and *Msr1* show also strong expression in extra-aortic macrophages (Fig. 4A).

### 4.3. Validation of RNA-seq target candidates with multifaceted complementary approaches

Although RNA-seq is a powerful tool that enables high-throughput assessment of thousands of gene regulations from one sample, validation of the chosen candidates is crucial owing to the fact that transcriptome does not perfectly stand for proteome. In this article, we deployed multifaceted tools to verify the expression of *Gpnmb* in atheroma, intending to demonstrate the potential of using RNA-seq data to identify targets of interest. Real-time PCR confirmed the quantitative accuracy of *Gpnmb* expression captured by RNA-seq (Supplementary Fig. 8A). Published scRNA-seq datasets allowed us to have a glimpse of *Gpnmb* expression in a wide-range of cell types as well as subtypes of macrophages. Knowing that *Gpnmb* is primarily expressed in a subset of foamy macrophages, we confirmed its positive association with atheroma aggravation. In line, we detected *Gpnmb* protein in a subset of atheromatous plaque macrophages by histology, and we detected a continuous rise in plasma *Gpnmb* levels as disease progressed (Supplementary Fig. 8B). However, the atheroma single-cell expression data document that *Gpnmb* is also expressed by fibroblasts besides macrophages, and therefore global *Gpnmb* deficiency or *Gpnmb* silencing experiments may not adequately and selectively explore the specific role of *Gpnmb*$^{+}$ macrophages in atherogenesis. Till the time when we composed this article, the role of *Gpnmb* in inflammation remains debatable and is well summarized in a recent review [27]. Some evidence suggests that Gpnmb supports inflammation resolution, while others demonstrate that Gpnmb could act pro-inflammatory, associating with enlarged plaque size specifically at the aortic roots in Apoe-deficient mice [54]. Using *Gpnmb* as a marker to distinguish *Gpnmb*$^{+}$ and *Gpnmb*$^{-}$ foamy macrophages, we were able to confirm that the latter express relatively high levels of inflammatory genes, and thus challenge the simplistic view that foam cells are non-inflammatory, as was previously suggested [55]. With the facilitation of RNA-seq datasets, we have gained precious knowledge for the future research, and we hope that our directory will be of value for the community in the search of regulators of monocyte and macrophage biology and potential therapeutic targets in the context of atherosclerosis.

**Financial support**

This work was supported by the Foundation of Studying Civilization Diseases to I.H., the German Research Foundation (HI1573/2, HI1573/9, HI1573/10). I.H. is a member of the Collaborative Research Centre SFB1425 (grant 422681845).

## Author contributions

CH acquired, analyzed and interpreted the data, and assisted in writing the manuscript, AK, CAE, TV, CS, AE, KK, BD, NH acquired and analyzed data. PS, TH, DW, CzM, BG, CSR, LM, DW provided materials and helped to interpreted the data and to edit the manuscript. TD and IH conceived and supervised the project, analyzed and interpreted the data, wrote the manuscript, and acquired funding.

## Declaration of competing interest

The authors declare that they have no known competing financial interests or personal relationships that could have appeared to influence the work reported in this paper.

## Acknowledgements

We thank staff members of the Lighthouse core facility at University of Freiburg, Marie Follo, Jan Bodinek-Wersing, and Dieter G. Herchenbach, for their help and guidance with cell sorting. We thank Vladimir Benes, Head of Genomic Core EMBL, Heidelberg, for his support and advice with sequencing.

## Appendix A. Supplementary data

Supplementary data to this article can be found online at https://doi.org/10.1016/j.atherosclerosis.2023.03.006.

## References

[1] G.K. Hansson, A.-K.L. Robertson, C. Söderberg-Nauclér, INFLAMMATION AND ATHEROSCLEROSIS [Internet], Annu. Rev. Pathol. 1 (1) (2006 Jan 24) 297–329, https://doi.org/10.1146/annurev.pathol.1.110304.100100. Available from:.
[2] I. Hilgendorf, F.K. Swirski, C.S. Robbins, Monocyte fate in atherosclerosis, Arterioscler. Thromb. Vasc. Biol. 35 (2) (2015).
[3] M. Mehu, C.A. Narasimhulu, D.K. Singla, Inflammatory Cells in Atherosclerosis, vol. 11, Antioxidants, 2022.
[4] P. Libby, Inflammation in atherosclerosis [Internet], Nature 420 (6917) (2002) 868–874, https://doi.org/10.1038/nature01323. Available from:.
[5] H. Itabe, Oxidative modification of LDL: its pathological role in atherosclerosis, Clin. Rev. Allergy Immunol. 37 (1) (2009).
[6] D. Mauricio, E. Castelblanco, N. Alonso, Cholesterol and Inflammation in Atherosclerosis: an Immune-Metabolic Hypothesis, vol. 12, Nutrients, 2020.
[7] A. Tsoupras, R. Lordan, I. Zabetakis, Inflammation, Not Cholesterol, Is a Cause of Chronic Disease, vol. 10, Nutrients, 2018.
[8] D. Hashimoto, A. Chow, C. Noizat, P. Teo, M.B. Beasley, M. Leboeuf, et al., Tissue-resident macrophages self-maintain locally throughout adult life with minimal contribution from circulating monocytes, Immunity 38 (4) (2013).
[9] S. Yona, K.W. Kim, Y. Wolf, A. Mildner, D. Varol, M. Breker, et al., Fate mapping reveals origins and dynamics of monocytes and tissue macrophages under homeostasis, Immunity 38 (1) (2013).
[10] C. Cochain, E. Vafadarnejad, P. Arampatzi, J. Pelisek, H. Winkels, K. Ley, et al., Single-cell RNA-seq reveals the transcriptional landscape and heterogeneity of aortic macrophages in murine atherosclerosis, Circ. Res. 122 (12) (2018).
[11] J.W. Williams, K. Zaitsev, K.W. Kim, S. Ivanov, B.T. Saunders, P.R. Schrank, et al., Limited proliferation capacity of aortic intima resident macrophages requires monocyte recruitment for atherosclerotic plaque progression, Nat. Immunol. 21 (10) (2020).
[12] H. Winkels, E. Ehinger, M. Vassallo, K. Buscher, H.Q. Dinh, K. Kobiyama, et al., Atlas of the immune cell repertoire in mouse atherosclerosis defined by single-cell RNA-sequencing and mass cytometry, Circ. Res. 122 (12) (2018).
[13] A. Zernecke, H. Winkels, C. Cochain, J.W. Williams, D. Wolf, O. Soehnlein, et al., Meta-analysis of Leukocyte Diversity in Atherosclerotic Mouse Aortas, vol. 127, Circulation Research, 2020.
[14] S.M. Eken, H. Jin, E. Chernogubova, Y. Li, N. Simon, C. Sun, et al., MicroRNA-210 enhances fibrous cap stability in advanced atherosclerotic lesions, Circ. Res. 120 (4) (2017).
[15] F. Fasolo, H. Jin, G. Winski, E. Chernogubova, J. Pauli, H. Winter, et al., Long noncoding RNA MIAT controls advanced atherosclerotic lesion formation and plaque destabilization, Circulation 144 (19) (2021).
[16] R.C. Wirka, D. Wagh, D.T. Paik, M. Pjanic, T. Nguyen, C.L. Miller, et al., Atheroprotective roles of smooth muscle cell phenotypic modulation and the TCF21 disease gene as revealed by single-cell analysis, Nat. Med. 25 (8) (2019).
[17] J. Leipner, T.S. Dederichs, A. von Ehr, S. Rauterberg, C. Ehlert, J. Merz, et al., Myeloid cell-specific Irf5 deficiency stabilizes atherosclerotic plaques in *Apoe*–/– mice, Mol. Metabol. (2021;53(May) 1–11.
[18] C. Härdtner, J. Kornemann, K. Krebs, C.A. Ehlert, A. Jander, J. Zou, et al., Inhibition of macrophage proliferation dominates plaque regression in response to cholesterol lowering [Internet], Basic Res. Cardiol. 115 (6) (2020) 1–19, https://doi.org/10.1007/s00395-020-00838-4. Available from:.
[19] C.S. Robbins, I. Hilgendorf, G.F. Weber, I. Theurl, Y. Iwamoto, J.L. Figueiredo, et al., Local proliferation dominates lesional macrophage accumulation in atherosclerosis, Nat. Med. 19 (9) (2013).
[20] J. Lee, J.H. Choi, Deciphering Macrophage Phenotypes upon Lipid Uptake and Atherosclerosis, vol. 20, Immune Network, 2020.
[21] N.J. Spann, L.X. Garmire, J.G. McDonald, D.S. Myers, S.B. Milne, N. Shibata, et al., Regulated accumulation of desmosterol integrates macrophage lipid metabolism and inflammatory responses, Cell 151 (1) (2012).
[22] D. Wang, W. Wang, W. Lin, W. Yang, P. Zhang, M. Chen, et al., Apoptotic cell induction of miR-10b in macrophages contributes to advanced atherosclerosis progression in ApoE2/2mice, Cardiovasc. Res. 114 (13) (2018).
[23] F.K. Swirski, M. Nahrendorf, M. Etzrodt, M. Wildgruber, V. Cortez-Retamozo, P. Panizzi, et al., Identification of splenic reservoir monocytes and their deployment to inflammatory sites, Science 80 (5940) (2009) 325.
[24] E. Adiguzel, P.J. Ahmad, C. Franco, M.P. Bendeck, Collagens in the Progression and Complications of Atherosclerosis, vol. 14, Vascular Medicine, 2009.
[25] A. Lindau, C. Härdtner, S.P. Hergeth, K.D. Blanz, B. Dufner, N. Hoppe, et al., Atheroprotection through SYK inhibition fails in established disease when local macrophage proliferation dominates lesion progression, Basic Res. Cardiol. 111 (2) (2016).
[26] A. Matsumoto, M. Naito, H. Itakura, S. Ikemoto, H. Asaoka, I. Hayakawa, et al., Human macrophage scavenger receptors: primary structure, expression, and localization in atherosclerotic lesions, Proc. Natl. Acad. Sci. U. S. A. 87 (23) (1990).
[27] M. Saade, G. Araujo de Souza, C. Scavone, P.F. Kinoshita, The role of GPNMB in inflammation, Front. Immunol. 1–10 (2021;12(May).
[28] J.X. Binder, S. Pletscher-Frankild, K. Tsafou, C. Stolte, S.I. O'Donoghue, R. Schneider, et al., COMPARTMENTS: unification and visualization of protein subcellular localization evidence, Database 2014 (2014).
[29] L. Willemsen, M.P.J. de Winther, Macrophage subsets in atherosclerosis as defined by single-cell technologies, J. Pathol. 250 (2020).
[30] C. Cochain, A.E. Saliba, A. Zernecke, Letter by Cochain et al regarding article, "Transcriptome analysis reveals nonfoamy rather than foamy plaque macrophages are proinflammatory in atherosclerotic murine models, vol. 123, Circulation Research, 2018.
[31] G. Chinetti, S. Lestavel, V. Bocher, A.T. Remaley, B. Neve, I.P. Torra, et al., PPAR-α and PPAR-γ activators induce cholesterol removal from human macrophage foam cells through stimulation of the ABCA1 pathway, Nat. Med. 7 (1) (2001).
[32] Alsaigh T, Evans D, Frankel D, Torkamani A. Decoding the transcriptome of atherosclerotic plaque at single-cell resolution. bioRxiv [Internet]. 2020 Jan 1; 2020.03.03.968123. Available from: http://biorxiv.org/content/early/2020/03/04/2020.03.03.968123.abstract.
[33] P. Libby, Inflammation in atherosclerosis, Arterioscler. Thromb. Vasc. Biol. 32 (9) (2012).
[34] I. Tabas, K.E. Bornfeldt, Macrophage phenotype and function in different stages of atherosclerosis, Circ. Res. 118 (4) (2016).
[35] T. Weinberger, D. Esfandyari, D. Messerer, G. Percin, C. Schleifer, R. Thaler, et al., Ontogeny of arterial macrophages defines their functions in homeostasis and inflammation, Nat. Commun. 11 (1) (2020).
[36] C.J. Kim, J.C. Khoo, K. Gillotte-Taylor, A. Li, W. Palinski, C.K. Glass, et al., Polymerase chain reaction-based method for quantifying recruitment of monocytes to mouse atherosclerotic lesions in vivo: enhancement by tumor necrosis factor-α and interleukin-1β, Arterioscler. Thromb. Vasc. Biol. 20 (8) (2000).
[37] S.M. Lessner, H.L. Prado, E.K. Waller, Z.S. Galis, Atherosclerotic lesions grow through recruitment and proliferation of circulating monocytes in a murine model, Am. J. Pathol. 160 (6) (2002).
[38] F.K. Swirski, M.J. Pittet, M.F. Kircher, E. Aikawa, F.A. Jaffer, P. Libby, et al., Monocyte accumulation in mouse atherogenesis is progressive and proportional to extent of disease, Proc. Natl. Acad. Sci. U. S. A. 103 (27) (2006).
[39] Y. Yan, M. Thakur, E.P.C. van der Vorst, C. Weber, Y. Döring, Targeting the Chemokine Network in Atherosclerosis, vol. 330, Atherosclerosis, 2021.
[40] F. Porsch, M.G. Kiss, L. Goederle, T. Hendrikx, A. Hladik, S. Knapp, et al., Haematopoetic TREM2 deficiency modulates atherosclerosis and lipid metabolism, Atherosclerosis (2020) 315.
[41] A.V. Poznyak, N.G. Nikiforov, A.V. Starodubova, T.V. Popkova, A.N. Orekhov, Macrophages and Foam Cells: Brief Overview of Their Role, Linkage, and Targeting Potential in Atherosclerosis, vol. 9, Biomedicines, 2021.
[42] J Da Lin, H. Nishi, J. Poles, X. Niu, C. Mccauley, K. Rahman, et al., Single-cell analysis of fate-mapped macrophages reveals heterogeneity, including stem-like properties, during atherosclerosis progression and regression, JCI insight 4 (4) (2019).
[43] M.A.C. Depuydt, K.H.M. Prange, L. Slenders, T. Örd, D. Elbersen, A. Boltjes, et al., Microanatomy of the human atherosclerotic plaque by single-cell transcriptomics, Circ. Res. 127 (11) (2020).
[44] W. Gu, Z. Ni, Y.Q. Tan, J. Deng, S.J. Zhang, Z.C. Lv, et al., Adventitial cell atlas of wt (wild type) and ApoE (apolipoprotein E)-Deficient mice defined by single-cell RNA sequencing, Arterioscler. Thromb. Vasc. Biol. 39 (6) (2019).
[45] M. Sharma, M.P. Schlegel, M.S. Afonso, E.J. Brown, K. Rahman, A. Weinstock, et al., Regulatory T cells license macrophage pro-resolving functions during atherosclerosis regression, Circ. Res. 127 (3) (2020).
[46] D.A. Chistiakov, A.A. Melnichenko, A.V. Grechko, V.A. Myasoedova, A.N. Orekhov, Potential of Anti-inflammatory Agents for Treatment of Atherosclerosis, vol. 104, Experimental and Molecular Pathology, 2018.

[47] P.M. Ridker, B.M. Everett, T. Thuren, J.G. MacFadyen, W.H. Chang, C. Ballantyne, et al., Antiinflammatory therapy with canakinumab for atherosclerotic disease, N. Engl. J. Med. 377 (12) (2017).
[48] J.-C. Tardif, S. Kouz, D.D. Waters, O.F. Bertrand, R. Diaz, A.P. Maggioni, et al., Efficacy and safety of low-dose colchicine after myocardial infarction, N. Engl. J. Med. 381 (26) (2019).
[49] A. Minty, P. Chalon, J.M. Derocq, X. Dumont, J.C. Guillemot, M. Kaghad, et al., Interleukin-13 is a new human lymphokine regulating inflammatory and immune responses, Nature 362 (6417) (1993).
[50] J. Schmitz, A. Owyang, E. Oldham, Y. Song, E. Murphy, T.K. McClanahan, et al., IL-33, an interleukin-1-like cytokine that signals via the IL-1 receptor-related protein ST2 and induces T helper type 2-associated cytokines, Immunity 23 (5) (2005).
[51] S. Kuchibhotla, D. Vanegas, D.J. Kennedy, E. Guy, G. Nimako, R.E. Morton, et al., Absence of CD36 protects against atherosclerosis in ApoE knock-out mice with no additional protection provided by absence of scavenger receptor A I/II, Cardiovasc. Res. 78 (1) (2008).
[52] K.J. Moore, V.V. Kunjathoor, S.L. Koehn, J.J. Manning, A.A. Tseng, J.M. Silver, et al., Loss of receptor-mediated lipid uptake via scavenger receptor A or CD36 pathways does not ameliorate atherosclerosis in hyperlipidemic mice, J. Clin. Invest. 115 (8) (2005) 2192–2201.
[53] K.J. Woollard, F. Geissmann, Monocytes in atherosclerosis: subsets and functions, Nat. Rev. Cardiol. 7 (2010).
[54] B. Nickl, F. Qadri, M. Bader, Role of Gpnmb in atherosclerosis of female mice, Biochem. Biophys. Res. Commun. 621 (2022 Sep) 20–24.
[55] K. Kim, D. Shim, J.S. Lee, K. Zaitsev, J.W. Williams, K.W. Kim, et al., Transcriptome analysis reveals nonfoamy rather than foamy plaque macrophages are proinflammatory in atherosclerotic murine models, Circ. Res. 123 (10) (2018).